Plasma Phys. Control. Fusion **42** (2000) B293–B310. Printed in the UK PII: S0741-3335(00)17897-2

Comparison of tokamak behaviour with tungsten and low-Z plasma facing materials

V Philipps†, R Neu‖, J Rapp†, U Samm†, M Tokar†, T Tanabe‡ and M Rubel§

† Forschungszentrum Jülich, Institut für Plasmaphysik, D-52425 Jülich, Germany, Association Euratom-KFA
‡ Center for Integrated Research (CIRCE), Nagoya University, Japan
§ Alfven Laboratory, Royal Institute of Technology, SE-100 44 Stockholm, Sweden, Association Euratom-NFR
‖ Max Planck Institut für Plasmaphysik, Garching, Germany, Association Euratom-IPP

Received 16 June 2000

Abstract. Graphite wall materials are used in present day fusion devices in order to optimize plasma core performance and to enable access to a large operational space. A large physics database exists for operation with these plasma facing materials, which also indicate their use in future devices with extended burn times. The radiation from carbon impurities in the edge and divertor regions strongly helps to reduce the peak power loads on the strike areas, but carbon radiation also supports the formation of MARFE instabilities which can hinder access to high densities. The main concerns with graphite are associated with its strong chemical affinity to hydrogen, which leads to chemical erosion and to the formation of hydrogen-rich carbon layers. These layers can store a significant fraction of the total tritium fuel, which might prevent the use of these materials in future tritium devices. High-Z plasma facing materials are much more advantageous in this sense, but these advantages compete with the strong poisoning of the plasma if they enter the plasma core. New promising experiences have been obtained with high-Z wall materials in several devices, about which a survey is given in this paper and which also addresses open questions for future research and development work.

1. Introduction

During the last two decades of fusion research, all fusion devices, with few exceptions, have implemented low-Z carbon based materials as plasma facing materials. This has improved the performance of these devices, significantly contributing to the steady increase of the fusion triple product of density, temperature and energy confinement. Optimization of the core plasma performance was the main driver for the use of graphite and a large operational database exists for these materials, which allows a reasonable prediction of the global plasma performance for future devices. Graphite materials are used, in general, in combination with special wall conditioning procedures like boronization, siliconization, lithium injection or beryllium evaporation [1–4], which reduce the oxygen impurities and improve the density control.

However, the development of fusion energy needs an integrated approach where several requirements have to be fulfilled simultaneously. While the contamination of the core plasma by impurities released from the wall must be kept below a critical level ($Z_{\mathrm{eff}} < 1.6$) [5], the plasma facing components have to withstand the α-particles and external heating power,

0741-3335/00/SB0293+18$30.00 © 2000 IOP Publishing Ltd

including off-normal events such as high heat loads from disruptions or runaway electrons. Furthermore, the α-particles have to be exhausted efficiently.

Plasma conditions and wall materials must also enable a sufficient lifetime of the first wall components for economic reasons. One of the most critical is the long-term retention of the radioactive tritium. The total amount of retained tritium has to be limited and controlled for reasons of fuel supply, safety, licensing and public acceptance of fusion energy [5].

The concerns about graphite materials are related to the latter points and, generally speaking, are coupled with its chemical interaction with hydrogen and oxygen. Chemical erosion leads to significant erosion yields even under low-temperature, cold plasma conditions and can seriously limit the lifetime under special conditions. Since the tokamak is a fairly closed system, most of the eroded material will be redeposited somewhere inside the machine. In order to minimize the net-erosion and optimize the lifetime of wall components, the redeposition should be concentrated in areas of major erosion. However, a significant fraction of carbon migrates long distances and finally forms thick deposits on special locations. These deposits are hydrogen rich and, as the tritium experiments in JET and TFTR have undoubtedly demonstrated, contain a major fraction of the total tritium fuel supplied to the machines on a long-term scale (10–20% of the total supply) [6, 7]. Extrapolation of the fuel retention to a steady-state burning fusion plasma is difficult. Nevertheless, we have to be aware that tritium retention might become unacceptable and will not allow the operation of the device with tritium on a longer time schedule. This is a very serious concern and urgently calls for the exploration of techniques to control the formation of the carbon deposits, their tritium uptake and, also, to reconsider the choice of plasma facing components in general.

The most promising alternative category of plasma facing materials are the high-Z materials. These materials have acceptable thermomechanical properties, the possible advantage of very low or negligible erosion at low plasma temperatures and a moderate uptake of tritium. These advantages compete with their strong poisoning effect of the plasma due to cooling by radiation losses, if the suppression of impurity release fails and/or impurity transport leads to accumulation in the central plasma. In general, high-Z wall materials allow only a narrow operational space compared to operation with graphite walls. Although interesting new experiences have recently been obtained with high-Z wall materials in several devices [8–15] the present database is not such that its use on a large scale in future devices such as ITER is confirmed, which urgently calls for more experiments in present devices, since tungsten is the ITER reference material for the divertor baffles.

2. Fusion plasma operation with low-Z plasma facing components

Low-Z plasma facing materials such as graphite, boron or beryllium are preferred as plasma facing materials since their ions are fully stripped in the plasma core. This leads to a negligible contribution of line radiation and energy is lost only by Bremsstrahlung ($\approx Z^2$), as demonstrated in figure 1. Present experiments show that the carbon impurity concentration in the plasma core decreases with density reaching a level of about 1% at the Greenwald density limit. Figure 2 shows, for example, the carbon core concentrations of TEXTOR and TEXTOR-94 Upgrade as a function of the line averaged density. At high densities the fuel dilution and radiation losses from carbon at core concentrations are tolerable, even if they are extrapolated to ITER [16, 5].

The possible limitations to achieving high plasma performance with a carbon wall may be caused by the formation of MARFE instabilities at the plasma edge [17–19]. A MARFE is a region of cold dense plasma. In limiter plasmas, such as TEXTOR-94, MARFEs occur only on the high-field side and in diverted plasmas they mainly occur in the X-point region. The instability develops at a critical density when the radiation losses from the MARFE region

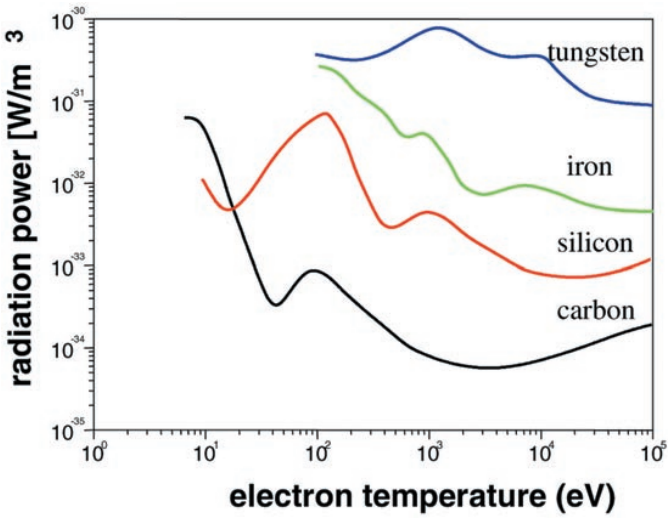

Figure 1. Total radiation losses as function of temperature, calculated assuming corona equilibrium for different impurities. Data from [69].

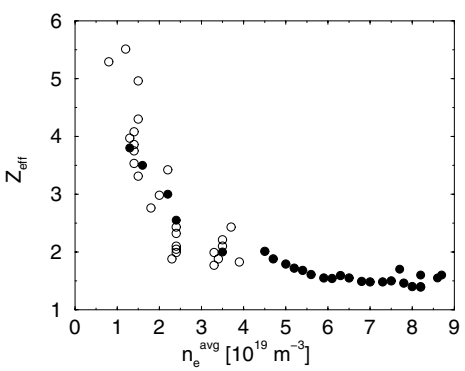

Figure 2. Central Z_{eff} of TEXTOR plasmas with graphite limiters and boronized wall conditioning depending on the plasma density. The full symbols are for 1.4 MW co-injection and the open symbols denote ohmic conditions.

cannot be compensated for by the power flow into it. A MARFE normally acts like a local charged particle pump, inhibiting the further increase of the average plasma density. TEXTOR-94 experiments have shown [20] that the critical density at which MARFEs start to grow can be shifted to higher values by increasing the distance between the plasma column and the wall on the high-field side or, at a normal plasma position, if the wall is freshly coated with silicon or boron. This demonstrates that the local release of impurities at the inner wall plays an important role and that the characteristics of chemical hydrocarbon release with erosion yields that are nearly independent of the impact energy is an important property.

In divertor machines MARFEs are formed deep inside the divertor, but can then rapidly move towards the X-point. This leads to a reduction of the plasma temperature, pressure and confinement and often ends in a disruption [3, 17]. MARFEs are critical for the achievement

of high densities with good confinement, and carbon impurities play a key role in their development, particularly in its early stage. Calculations show that inside a MARFE the plasma temperature can decrease and the density increase such that hydrogen radiation by recombination becomes important.

While carbon radiation can lower the critical density for MARFE formation, its radiation from the edge and inside the divertor can significantly reduce the peak power fluxes to the divertor strike zones. A large contribution to the radiation level from the divertor volume requires a low-Z radiator such as carbon [21]. Experiments in ASDEX Upgrade have shown that a radiation level of 80% can be achieved independently of the input power and that about half of this is radiated within the divertor volume. The radiation shows a stabilizing, feedback-like behaviour, with higher radiation when the power flux crossing the LCFS is increased [22]. The radiation characteristics and the chemical erosion behaviour of the carbon (which is nearly independent of the plasma temperature) are essential for this stabilizing effect. About two-thirds of the total radiation is from carbon impurities.

However, the operational window between the high radiation levels in the divertor, which lead to (partial) detached plasma states and MARFE formation, and the degradation of the main plasma performance remains a critical issue, and is different for different devices. This behaviour is not yet fully understood but is of particular importance for extrapolation to ITER [23]. In general, despite some promising results, the simultaneous achievement of high divertor radiation and good H-mode energy confinement has not been demonstrated with a sufficient degree of confidence in the present large divertor devices.

3. Erosion behaviour of carbon-based wall materials

The greatest advantage of graphite is that it does not melt under off-normal heat loads. The biggest concern with graphite is related to erosion under normal operation.

The physical sputtering of graphite by D impact reaches the 1% level at plasma temperatures above about 15 eV and is below about 10^{-3} only for plasma temperatures below about 5 eV. Chemical erosion by hydrocarbon formation dominates the carbon influx for most of the plasma edge conditions. Chemical erosion of carbon by hydrogen impact is a complex process, the atomistic mechanisms of which are only partly clarified [24–26].

The chemical formation rates depend on the target temperature, the particle impact energies and fluxes and on the surface condition of the carbon material. For low flux densities ($<10^{19}$ (m^2 s^{-1})) and high impact energies (>200 eV) the yields at the maximum temperature (800–900 K) increase up to 10–15% and the yield is below 5×10^{-3} at a cold target. When the impact energy decreases, the yield at the maximum temperature (600–1000 K) decreases with values of around 3–5% at 10–20 eV, but, surprisingly, the yield increases for target temperatures below 400 K. At plasma temperatures of 10–20 eV the dependence on the target temperature is flat.

The chemical erosion behaviour by the impact of thermal hydrogen atoms ($E = 0.2$ eV) shows the importance of the surface condition of the graphite material. As can be seen in figure 3, chemical yields above 10% at the maximum temperature are reached for thermal atom impact on amorphous hydrocarbon films, but the yield is only about 10^{-3} for undamaged well ordered graphite [27]. The yields are also large for redeposited carbon taken from TEXTOR or for pyrolytic graphite, which has previously been damaged by energetic ion beam irradiation. At the maximum temperature the yields reach, or even exceed, the values of energetic ion impact (at lower energies) on undamaged graphite surfaces. Similar to this behaviour, the simultaneous impact of thermal atoms together with a small high-energy component (hydrogen or other ions) results in a large enhancement of the erosion of the thermal component, called

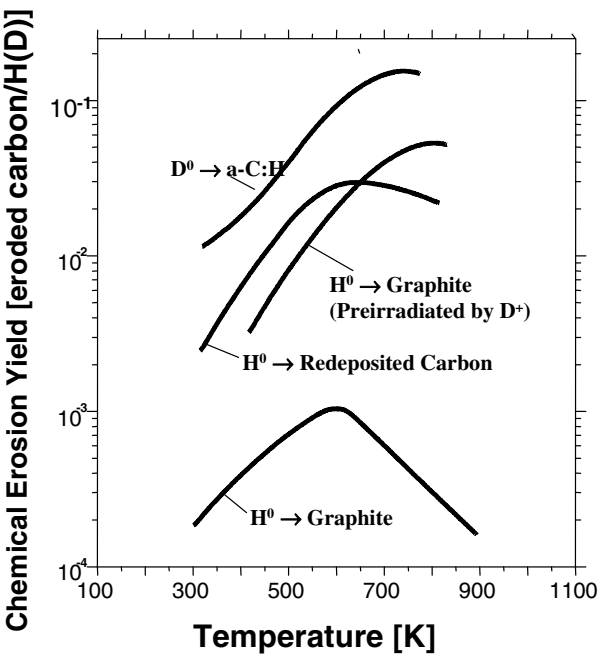

Figure 3. Erosion behaviour of different types of carbon material under the impact of hydrogen atoms with thermal energy of 0.2 eV.

'synergistic erosion' [28]. The synergistic enhancement depends on the energy of the energetic ion component and the flux ratio of atoms and energetic ions [29]. Figure 4 shows a spectrum of the hydrocarbon species formed by thermal impact on 'hard' a-C:H films at a temperature of 570 K. The overall erosion is dominated by higher hydrocarbons. This is consistent with ion beam data, which show that the amount of higher hydrocarbons increases with decreasing particle impact energy. At low impact energies, as in fusion devices (<100 eV), at least equal amounts of C_1H_x and C_2H_y have to be considered, which is in fact estimated from optical and mass spectroscopic observations in tokamaks [30–33]. Under cold divertor conditions, C_2H_y formation dominates the graphite erosion, particularly if the surface of the target is in a deposition dominated regime.

An important question is the chemical erosion yield at the high flux densities which occur at the strike zones in fusion devices. In the lower flux range of up to several 10^{22} D $(m^2\ s)^{-1}$ only a weak tendency of decreasing yields with increasing flux densities is observed [26]. For higher fluxes the data are based on the spectroscopy of the CH radical in front of limiters and divertor plates, which then have to be translated into absolute fluxes using the CH photon efficiency. At the higher impact energies on the limiters (>200 eV) the yield is about constant, at around 3–4%, up to fluxes of $(3–5)10^{22}$ $(m^2\ s)^{-1}$, but decreases for higher fluxes. In the divertor for similar flux conditions, but lower energies, the experiments show a strong decrease of the CH light emission; but the translation into absolute fluxes is difficult due to the strong dependence of the CH photon efficiency on the plasma parameters in this regime [34, 35]. However, several experiments conclude that a strong decrease of the chemical erosion is obtained. Certainly, additional experiments are necessary to confirm this.

If carbon impurities are deposited at low energies (<50 eV), so-called 'soft like' carbon

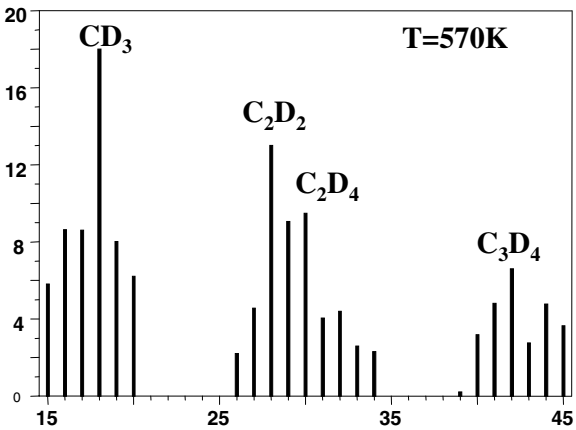

Figure 4. A spectrum of hydrocarbons formed by the impact of hydrogen atoms with a thermal energy of 0.2 eV on amorphous hydrocarbon films (diamond like carbon).

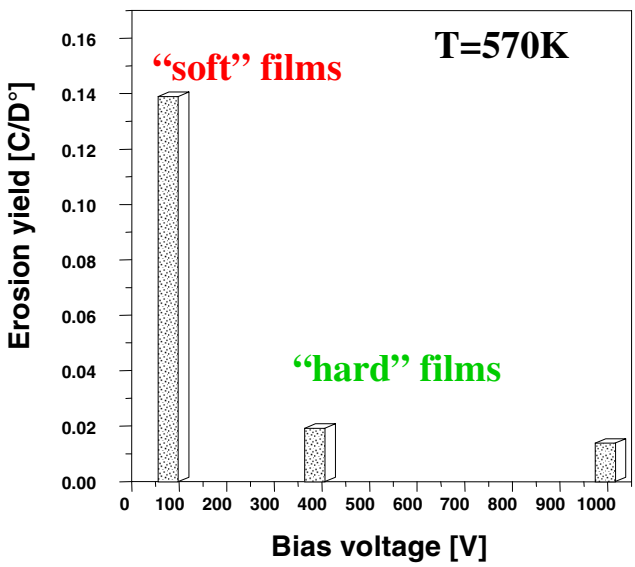

Figure 5. Total chemical erosion rates of different kind of carbon films (hard and soft) by the impact of hydrogen atoms with thermal energy. The temperature is 570 K.

layers are formed, characterized, for example, by a larger hydrogen content, smaller densities and a smaller refraction coefficient compared with hard films. Soft carbon films show strong chemical erosion under thermal hydrogen impact, which can exceed those of hard films by up to a factor of ten. This is shown in figure 5 for a target temperature of 570 K [36]. For higher temperatures ($\gtrsim$600 K) the films already dissolve in a large family of higher hydrocarbons [37] and no real erosion yield can be obtained since the erosion occurs in parallel with thermal decomposition. The formation of soft films in cold divertor plasmas is probably a mechanism similar to that which determines carbon release and transport in the divertor, as discussed in

more detail in section 6.

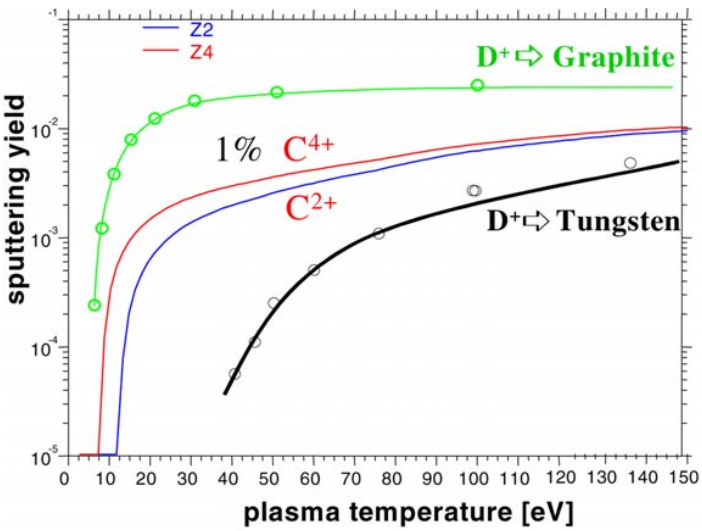

Figure 6. Calculated sputtering yield of tungsten by the impact of deuterium as a function of the plasma temperature. The impact energy is given by a Maxwellian energy distribution shifted by the sheath potential. The figure also shows the release rates if fluxes of 1% C^{2+} and C^{4+} are added to the deuterium flux. The data for the sputtering of carbon by deuterium impact is provided for comparison.

4. Erosion behaviour of high-Z materials

Physical sputtering occurs due to the removal of surface atoms by elastic collisions with projectiles, which results in yields that are, for light ion impact, roughly inversely proportional to the mass and the surface binding energy of the solid. In the case of deuterium impact on tungsten, this leads to low erosion yields with a large threshold energy towards low impact energies, as shown in figure 6. The figure also shows the corresponding release rates if a flux of 1% of C^{2+} or C^{4+} impurities is added to the deuterium flux. The impurity flux largely determines the erosion of tungsten, particularly at low plasma temperatures. Therefore the influx of the W impurities on areas determined by ion flux impact, such as the limiters or the divertor targets, is largely dominated by the impurity fraction of the deuterium flux, whereas in remote areas, in which the neutral hydrogen flux by charge exchange processes dominates, the erosion is given by the low yields of deuterium impact.

Figure 7 shows the measured effective W erosion yield as a function of the local plasma temperature on TEXTOR test limiters and on the ASDEX Upgrade outer divertor target, which were obtained using optical emission spectroscopy [38]. The TEXTOR data are obtained with the limiter 0.5 cm inside the radius defined by the main toroidal limiter and with 1.5 MW of neutral beam heating, resulting in power flux densities between about 8 and 15 MW m^2 [39]. The ASDEX Upgrade data include L-mode and H-mode conditions at various power flux densities. At the high plasma edge temperatures in TEXTOR yields as large as 3% are obtained, decreasing down to about 0.5% at the lowest temperatures. The C and O impurity fractions are between 4 and 2% and 2 and 1%, respectively, and decreasing with decreasing plasma temperature. The effective erosion yields in the ASDEX Upgrade outer divertor are

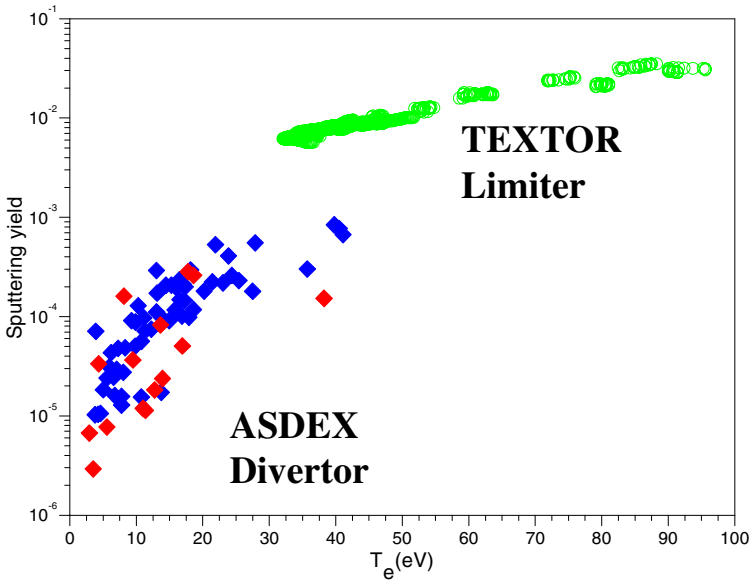

Figure 7. Measured effective W erosion yields on the outer ASDEX Upgrade tungsten divertor tile and on a tungsten test limiter in TEXTOR 94. The yields are evaluated from the WI line at 400.8 nm and the photon efficiencies are taken from [70].

between 10^{-5} and 10^{-3}. In TEXTOR and ASDEX Upgrade the tungsten release is dominated by low-Z impurity impact. The lower yields in ASDEX Upgrade are principally due to lower plasma temperatures, but the yields are also smaller at similar plasma temperatures. This can partly be explained by the stronger dilution of W in the target tiles of ASDEX Upgrade, which is up to 50% even in regions of net erosion in the outer divertor, and partly to different fractions of low C and O impurity fluxes [40]. In TEXTOR, the benefit of the low W erosion at the limiter is largely reduced by the low-Z impurity impact with the surrounding carbon wall that is in contact with comparable high edge temperatures. Low-Z impurity impact also dominates in the ASDEX Upgrade divertor, but the lower plasma temperatures help to reduce the effective yields.

The reduction of the edge temperatures in TEXTOR-94 by neon seeding reduces the erosion yields, but the overall tungsten release does not decrease as additional sputtering of tungsten by neon occurs. A substantial decrease of the overall tungsten release occurs under radiation improved confinement conditions (RI-mode) due to reduced particle fluxes to the limiters and, as an additional effect, due to plasma edge cooling [41]. However, the reduction of the high-Z source strength under the RI-mode conditions is overcompensated by an increase of the high-Z confinement times, as is described later in detail. In contrast, in ASDEX Upgrade the divertor neon seeding has resulted in a measurable decrease of the tungsten influx. This is due to the fact that the particle impact energies are in a region near the sputtering threshold where the yields vary steeply with energy [38].

Generally, in devices dominated by graphite walls, such as TEXTOR-94 and ASDEX Upgrade, the high-Z influx is increased largely by carbon sputtering. However, this also leads to carbon deposition decreasing W release, due to the partial coverage of the tungsten surface. Sometimes it can even suppress the high-Z erosion completely, as in the inner divertor of

ASDEX Upgrade or on limiter areas positioned deeper in the SOL of TEXTOR-94. When the wall area covered with graphite decreases, both the carbon fluxes and the carbon deposition will decrease. On the other hand, with a decrease of low-Z impurities the plasma temperature will increase because of lower radiation losses. This should result in an increase of the high-Z sputtering yields. These dependences illustrate the complexity of the system, where an estimate of the overall high-Z impurity influx has to be treated in a coherent way, taking into account all of these effects.

Alcator C-mod operates with a first wall and divertor tiles made entirely from molybdenum. Both the inner wall and the divertor contribute to the Mo-concentration in the main plasma. However, the penetration probability of Mo particles released from the divertor reaching the core plasma is small, and that of Mo released from the inner wall is only about 0.05. The dominant Mo source is on the RF antenna screens, which are close to the plasma and from which the Mo particles have a high penetration probability (close to unity) [42]. Under certain conditions Mo radiation from the core can deteriorate the plasma performance, which would be eliminated if the RF Mo source could be better controlled. However, the dominant impurity in the plasma is carbon and parts of the Mo tiles are covered with thick carbon coatings, which reduce the overall Mo influx. It is believed that a chemical interaction of hydrogen with the C impurities in the bulk of the Mo tiles liberate the C, leading to a progressive enrichment of the first wall surfaces with carbon coatings. To what degree a carbon free surrounding can be achieved in fusion devices is not yet clear.

On areas where the flux of neutrals from charge exchange (CX) hydrogen dominates and no or very low impurity ion fluxes exist (as on the baffle or on the main chamber wall), tungsten has the benefit of low sputter yields and a large threshold energy, for example for deuterium impact. An estimation of the tungsten release requires the determination of the flux and the energy distribution of the CX neutrals. Figure 8 shows the W influx for ASDEX Upgrade based on CX measurements and B2-EIRENE calculations [43]. The calculations are consistent with measurements in ASDEX Upgrade, in which W-coated graphite tiles were employed on a toroidal ring in the upper baffle region with a total area of about 1.2 m^2 [44]. The W influx was low and the concentration of W in the plasma was always below 5×10^{-6}. These are very encouraging results, suggesting the use of W on larger areas of the first wall. Extrapolation to ITER conditions show that the W core concentrations with a full tungsten wall are tolerable.

5. Graphite and high-Z erosion at high temperatures

Chemical erosion via hydrocarbons vanishes at high graphite temperatures. At the high fluxes achieved in tokamaks (10^{22}–10^{23} m^{-2} s^{-1}) the decrease of hydrocarbon formation is shifted towards higher temperatures (800–1100 K) compared to low fluxes [30]. This is also observed in beam experiments [26, 45].

In beam experiments at low flux densities, carbon materials show an additional sublimation of carbon atoms that dominates the overall erosion in the temperature region from about 1400 K up to the temperature of normal sublimation, called radiation enhanced sublimation (RES) [46, 47]. Observations in TEXTOR-94 [48] and JET [49] have shown that this erosion channel seems to be unimportant for those impact energies and high flux densities occurring at limiters and divertor targets. A possible enhancement of the carbon erosion above 1400 K due to RES at areas with lower flux densities is not yet clear. However, the temperatures of the wall areas in low-flux regions will be probably well below the critical temperature for the onset of RES.

The robustness of graphite to transient high heat loads during disruptions is the main reason for its use in divertor plates. An ITER disruption is expected to deposit 100 MJ m^2 over about 1 ms. Assuming that the width of the deposition is similar to that of present experiments,

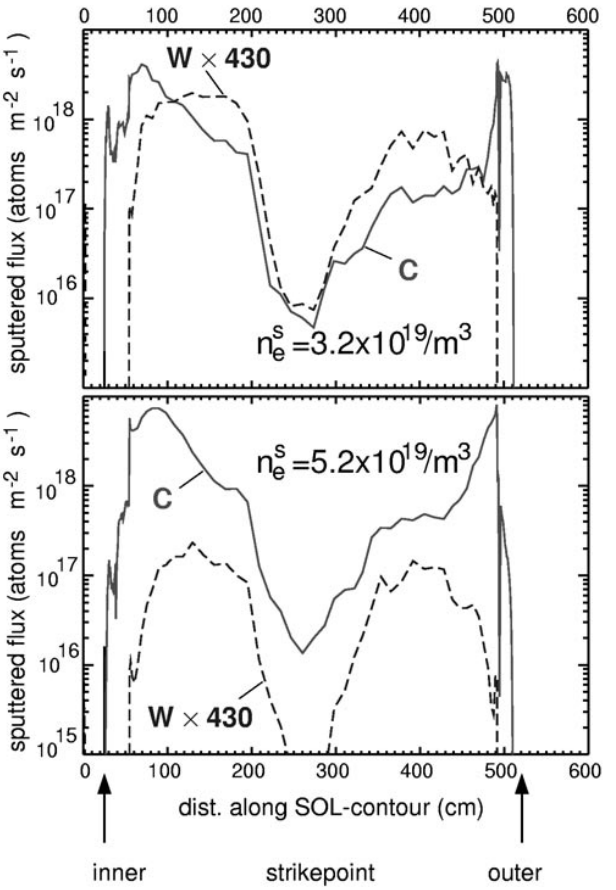

Figure 8. Calculated influx of W and C impurities from the first wall of ASDEX Upgrade. The data are based on measured CXS particle fluxes and energies and B2-Eirene calculations.

we obtain a power flux density of 100 GW m^{-2} on the divertor plates. Such heat loads result in vaporization, melt layer splashing or explosive erosion. Present results from calculations and experiments [5] show that for tungsten the melt layer reaches a thickness of the order of 100–200 μm and that the loss is about 15–75 μm per event. Graphite shows no melting, only sublimation, with the consequence that much less material is lost during a disruption. Recently, new results have been obtained on the erosion of graphite by the explosive emission of small particles; in view of which the criteria for the choice of the material at the divertor plates might have to be reconsidered. Although of considerable importance for the choice of first wall materials, a more detailed discussion of off-normal heat loads is out of the scope of this paper.

6. Low- and high-Z impurity penetration, material transport

Only a small fraction of the impurities produced can escape from a fusion device (for example, by pumping of volatile and non-reactive molecules); but for all other species the tokamak is a

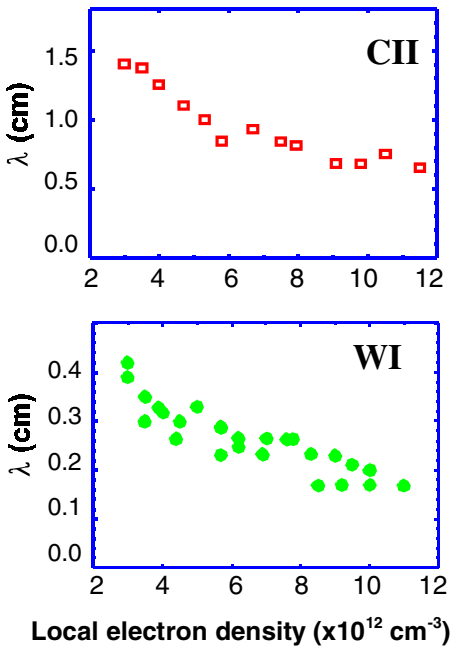

Figure 9. Measured penetration depths of W and C in front of W and C TEXTOR test limiters depending on local plasma density.

closed system and erosion and deposition occurs simultaneously in equal amounts. A fraction of the impurities is deposited in the vicinity of the region where they are eroded (local or prompt redeposition). The others enter the confined plasma and are deposited at other locations of the wall (global redeposition). These transport processes lead to material redistribution and, if different materials are used, to material mixing.

Local redeposition is determined by the penetration depths of the impurities, the local geometry of the target with respect to the magnetic field lines and the various forces acting on the ionized impurities, such as friction, thermal forces and electric fields. Figure 9 shows the measured penetration depths of the carbon and tungsten atoms released from a test limiter in TEXTOR as a function of the local plasma density. The high-Z impurities have a small penetration depth due to their low velocity as a result of their large mass. At the highest densities the penetration depths of Mo and W are close to or below 1 mm. The penetration depth of C is significantly larger and is related to C originating from physical sputtering and chemical erosion. However, the penetration depth of C originating from hydrocarbons is smaller compared to physically sputtered carbon [50].

When the penetration depth of the neutrals becomes as small as the ion Larmor radius, local redeposition is likely to occur within the first gyration of the ion. This effect is called prompt redeposition, and was first discussed in [51]. Table 1 shows the probabilities for the overall prompt and total redepositions of C and W atoms released from a test limiter in TEXTOR-94 under different plasma conditions and calculated with the local Monte Carlo code ERO-TEXTOR [52]. Under typical TEXTOR-94 conditions the calculated fraction of the prompt redeposition of W reaches values of up to 50%; but values of up to 90% are obtained for divertor plasma conditions [53, 54]. The prompt redeposition of W is difficult to quantify

experimentally. A qualitative confirmation of the calculations was obtained by comparing the relative change of the high-Z impurity content in the plasma with that of the local W release.

Table 1. Carbon and tungsten redeposition on TEXTOR limiters calculated with ERO-TEXTOR.

		Tungsten		Carbon	
T_e (LCFS) (eV),	n_e (LCFS) (cm^{-3})	Total redeposition (%)	Prompt redeposition (%)	Total redeposition (%)	Prompt redeposition (%)
40,	1×10^{12}	15	64	2	8
80,	1×10^{12}	23	72	2	20
40,	4×10^{12}	36	74	8	14
40,	9×10^{12}	49	72	19	15
80,	9×10^{12}	58	80	20	22

The transport and redeposition of methane was studied in TEXTOR-94 using methane injection through the limiters positioned at the LCFS [55]. A precisely known amount of methane was puffed through a test limiter and the amount and pattern of the redeposited carbon was compared to predictions from the ERO-TEXTOR code. Surprisingly, the local redeposition probability of the puffed methane is very small (less than 1%), in contrast to the code calculations based on the 'standard assumptions' for the chemical erosion of the deposited carbon film and for the sticking probability of the returning hydrocarbon fragments (0.5 for ions and zero for neutrals). The best assumption that could reasonably well match the amount and the pattern of the redeposited carbon and, simultaneously, the spatial distribution of the CH and C^+ light emission is a high chemical re-erosion probability of the freshly deposited carbon. The yields have to be at least one order of magnitude higher (≈20–30%) compared to the standard values used so far. An experiment with ^{13}C marked carbon atoms shows that the final deposition of carbon is on obstacles all over the whole wall. Thus, if the chemically released hydrocarbons produced in normal plasma wall contact behave in the same way (which has to be confirmed by further experiments), the carbon impurities migrate long distances and an enhanced material flow from areas of high particle fluxes to remote areas results. This assumption is at least in qualitative agreement with many observations on several fusion devices.

In TEXTOR-94, carbon layers have been found in the pump ducts of the toroidal pump limiter, where no plasma exists [59]. Furthermore, in ASDEX Upgrade carbon layers have been found behind the divertor targets on the divertor floor [44]. In JET, thick carbon layers (>200 μm) were formed within a short period of operation on the louvres at the entrance to the cryopump ducts [56]. This, also, cannot be explained using standard assumptions. As for the TEXTOR-94 methane puff experiments, the assumption of large erosion rates of more than 10% at the strike zones of the divertor target is a reasonable assumption in order to produce the flow of carbon needed to build up the layers observed. Alternatively, one can also assume a negligible sticking probability of all of the hydrocarbon fragments returning to the surface, which results in long-range transport via multistep processes and which, however, is not in agreement with measurements [58].

Erosion rates above 10% at low impact energies and of intermediate surface temperatures (400–600 K) are typical for soft carbon films, which also decompose totally into hydrocarbon fragments at slightly elevated temperatures (>600 K). Thus, it seems to be most likely that enhanced chemical erosion and thermal decomposition of freshly deposited soft carbon films are essential (the driving mechanism) for the formation of thick deposits on remote areas. More generally speaking, soft carbon films do not survive at the first location of

deposition and the carbon is transported finally to remote areas of low flux and/or low surface temperature.

In general, the main vessel wall and the limiter tip are areas of net erosion [58, 59]. Part of the eroded material is re-distributed onto limiters [60], but a large part migrates long distances and is deposited on obstacles or on the side walls of the limiters, where it forms thick layers with a hard and brittle structure. The average deposition rate in the SOL of TEXTOR-94 ($r = 50$ cm) is about 3–5 nm s^{-1}, which corresponds to unreasonably thick deposits of 0.12 m/year for steady-state operation. However, the deposits peel off when they reach a thickness in the micrometre range, finally forming dust at the floor of the device.

In a divertor, a fraction of the material is transported along the field lines into the divertor. There the material is first deposited at the strike zones and forms hydrogen-rich hard or soft films with the erosion properties described above; finally the material is transported to remote areas. In this general picture an important parameter for the carbon emission from the divertor target and, finally, for the carbon deposition on remote areas is the flux ratio of the C/H flowing down into the divertor. Not much data exist for this quantity, but an effective C/H yield at the inner divertor near or larger than 10% requires an equivalent C/H flux ratio flowing into the inner divertor; taking into account that the inner divertor targets show no net erosion and cannot thus deliver the necessary amount of carbon. Such a high impurity flux into the divertor cannot be explained with our present understanding of impurity production in the main chamber and indicates either a much stronger plasma contact with the wall and/or preferential impurity flows from the outer side to the inner side of the divertor. Indeed, observations show preferential flows in the SOL towards the inner divertor leg as well as enhanced plasma contact with the inner wall of the JET device [61].

7. Operation experiences with high-Z walls

Rather discouraging experiences with high-Z walls have been obtained in early experiments [62, 63]. An uncontrolled rise of the high-Z ion concentration in the plasma core occurred leading to strong radiation losses with hollow or flat temperature profiles which were often followed by a plasma disruption. Nowadays, high-Z materials are again being reconsidered due to the problems expected with the use of carbon. Some new operational experience has been obtained in FTU, Alcator-C-mod, ASDEX Upgrade and TEXTOR-94, which employ new heating methods in addition to ohmic heating.

In TEXTOR-94, as in the early observations on PLT [62], the accumulation of high-Z impurities occurred very reproducibly under pure ohmic heating conditions [8]. Although the W and Mo limiters were loaded with only a fraction of the total convective power, of about 4–6%, regular W and Mo accumulation occurred when a critical plasma density was reached (figure 10). The high-Z accumulation behaviour was very similar for the Mo and W limiters and was characterized by rapidly growing radiation from the plasma centre and the development of flat or hollow temperature profiles. In the first phase of the accumulation the W concentration rises slightly and shows a decrease of the sawtooth amplitude and temperature. This is followed by a phase in which the on-axis q exceeds unity. Then the sawtooth activity disappears, the increase of the high-Z impurity accelerates, the electron temperature rapidly decreases and a reversed q-profile develops in the central region. This leads to an internal disruption that is followed by a recovery period after which the accumulation can again occur [64]. Interestingly, the critical density for the onset of accumulation depends only weakly on the absolute amount of impurities released. This proves that the accumulation is driven by the internal impurity transport.

In auxiliary heated plasmas ($P > 1$ MW) accumulation did not occur (with a few

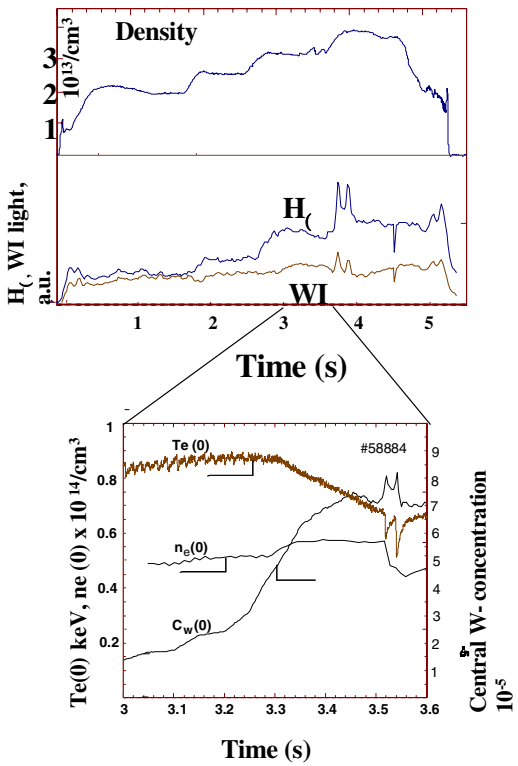

Figure 10. Time traces of electron temperature, density and core W concentration for a typical W accumulation in TEXTOR.

exceptions) in TEXTOR-94 operated with Mo and W test limiters or with a full set of poloidal limiters with a plasma-sprayed W layer (10 tiles covering about 20% of the poloidal circumference). However, the W concentration in the core reaches values of several 10^{-4} at medium electron densities ($n_e = 3$–4×10^{13} cm^{-3}) with a convective heat flux to the test limiter of typically (2–5)$\times10^{-2}$ of the total heat flux and a local W/H release ratio of about 2×10^{-2}. This indicates that a significant fraction of the released tungsten enters the confined plasma.

For a few cases with neutral beam injection (deuterium) W accumulation has been observed at low electron densities showing that the system can change into a state where accumulation can occur [66].

The concentration of W or Mo in the core decreases strongly with increasing density, resulting in high-Z impurity concentrations below the detection limit ($<10^{-5}$) at high densities. The edge cooling of the plasma with neon increases the high-Z impurity content in the plasma, which is attributed to an increase of the impurity confinement time. At intermediate densities, W accumulation occurs for such conditions at higher edge radiation levels (>65%), which was not observed for Mo limiters under similar conditions. The W accumulation with neutral beam injection develops similarly as for the ohmic case, but the W particles can stay in the core for a long time (>0.5 s) without any internal disruption. At high electron densities and high edge radiation, accumulation was not observed; this is due to a reduction of the W source together

with increased screening. Thus W accumulation is expected for a larger source, for example, like with larger areas covered with tungsten.

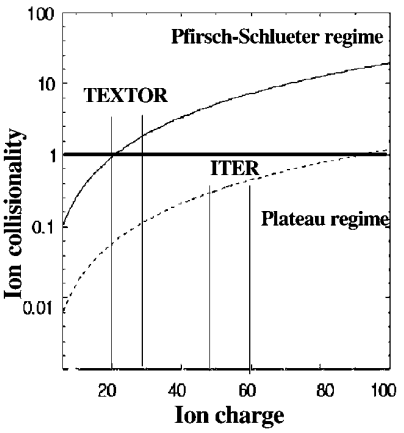

Figure 11. Collisionality of impurity ions in the plasma core of TEXTOR ($n_e = 6 \times 10^{13}$ cm^{-3}, $T_e = 1.5$ keV, $R_0 = 1.75$ m) and ITER ($n_e = 1.75 \times 10^{14}$ cm^{-3}, $T_e = 17$ keV, $R_0 = 8.3$ m).

In ASDEX Upgrade, copious investigations using W laser blow off showed no W accumulation except for unduly high amounts of injected W, which led to strong central cooling and a flattening of the temperature profile [54, 66]. During operation with a full set of tungsten divertor tiles no degradation of the operation limits and the confinement were observed, and in about 85% of all discharges the W concentration was below 2×10^{-5}, and even as low as 10^{-6} in high-power, high-density H-mode.

Accumulation occurred only in counter NI heating and with NI heating at low beam energies, leading occasionally to internal disruptions. However, it has to be stated here that under these discharge conditions, the accumulation of other intrinsic impurities was also observed. An increased confinement of W with neon seeding was also observed in ASDEX Upgrade. This effect is counteracted by a decrease of the W source in the divertor with neon cooling [67]. Recently, W-coated graphite tiles have been employed in ASDEX Upgrade on a toroidal ring in the upper baffle region with a total area of about 1.2 m^2. The concentration of W in the plasma was always below 5×10^{-6} and mostly below the detection limit. These are very encouraging results suggesting the use of W on larger areas of the first wall. Extrapolation to ITER conditions suggest that the expected tungsten core concentrations arising from the tungsten divertor baffles will be tolerable [11].

In FTU, high-Z accumulation is observed under ohmic conditions with the typical appearance of strong central radiation and hollow temperature profiles. No clear density threshold could be seen in this case, but the appearance of accumulation in the start-up phase could be avoided using a low ratio of I_p/n_e during the ramping-up phase of the plasma [12].

The accumulation of high-Z in the plasma core can be well explained in terms of neo-classical impurity transport [68]. The outward diffusive flow, which is mainly of an anomalous nature, is balanced by a convection which is driven by the neo-classical effects. The neo-classical convective flow consists of a part which is directed towards the centre and proportional to the density gradient of the background ions and a part which is proportional to the ion temperature gradient. In the collisional so-called Pfirsch–Schlüter regime the latter constituent

of the impurity flux is directed towards the edge and is thus responsible for the so-called temperature screening. A decrease of the on-axis temperature by an increase of the high-Z ion radiation in the plasma core thus leads to a reduction of the temperature screening and impurity flow to the axis due to the convection caused by the density gradient of the main ions. In this manner an instability can develop which leads to the observed high-Z accumulation.

At higher plasma temperatures, as for ITER, the collisionality decreases and the high-Z impurities are in the banana plateau transport regime. The regions with different transport regimes are shown in figure 11. In the collisionless plateau regime the neo-classical flows are directed towards the centre. This results, basically, in peaked impurity profiles, but the magnitude of the peaking is only moderate due to the flat density profiles and to the moderate amount of convective flow driven by the temperature gradient.

8. Summary

The main results of this work are as follows.

- **Carbon-based plasma facing materials**
  - * Plasma operation with a surrounding carbon wall leads to tolerable radiation and fuel dilution in the core at the high plasma densities necessary to achieve the criteria for efficient fusion conditions, even if extrapolated to ITER conditions at high densities ($n_e = 0.85\, n_{gr}$).
  - * Carbon impurities can radiate at low plasma temperatures in the divertor region and are essential in establishing high-density, partially-detached plasma conditions, which are necessary to reduce the peak power loads in future devices. The replacement of carbon would require the external seeding of impurities, which requires the use of nitrogen, if radiation should be kept substantially inside the divertor.
  - * Carbon radiation can trigger the formation of MARFE instabilities at a critical density and can hinder access to higher densities.
  - * Graphite does not melt and thus shows no melt layer loss in the case of severe disruptions.
  - * Large chemical erosion, even under very cold plasma conditions, trigger the deposition of thick carbon films on various areas, including remote areas which are difficult to access. These would store intolerably large amounts of tritium in future devices, and this is likely to prevent the use of carbon materials in devices using tritium.
- **High-Z plasma facing materials:**
  - * The release of high-Z impurities is largely determined by the amount of other low-Z impurities present, which can reduce the influx of high-Z impurities due to the covering of the surface with low-Z impurities, for example, carbon. Careful analysis is necessary before extrapolating small-scale high-Z experience in present carbon-dominated devices to a full high-Z walls.
  - * The accumulation of high-Z impurities is observed in all devices under certain operational conditions. The transport of high-Z impurities in the plasma core is one of the most critical issues in using these materials. Neo-classical fluxes can lead to a strong accumulation in the plasma centre, which can lead to a radiation collapse. The present predictions for ITER predict only a moderate peaking of high-Z impurities in the core region, which might be tolerable if the source can be kept low enough.

References

[1] Winter J *et al* 1989 *J. Nucl. Mater.* **162–164** 713
[2] Winter J *et al* 1993 *Phys. Rev. Lett.* **71** 1549
[3] Samm U *et al* 1995 *J. Nucl. Mater.* **220–222** 25
Samm U *et al* 1993 *Phys. Rev. Lett.* **71** 1549
[4] Campbell D 2000 *Nucl. Fusion* submitted
[5] Iter Physics Basis Editors 1999 *Nucl. Fusion* **39**
[6] Skinner C H and the TFTR team 1997 *J. Nucl. Mater.* **242–243** 214–26
[7] Andrew P *et al* 1999 *J. Nucl. Mater.* **266–269** 153
[8] Philipps V, Tanabe T and Ueda Y *et al* 1994 *Nucl. Fusion* **34** 1417
[9] Neu R *et al* 1996 *Plasma Phys. Control. Fusion* **38** A165
[10] Noda N, Neu R and Philipps V 1997 *J. Nucl. Mater.* **241–243** 227
[11] Neu R *et al* 2000 *14th Conf. on Plasma Surface Interactions (Rosenheim, Germany, May 2000) J. Nucl. Mater.* to be published
[12] Alladio F *et al* 1994 *Plasma Phys. Control. Fusion* **36** B253
[13] Apicella M L *et al* 1997 *Nucl. Fusion* **37** 381
[14] Lipschultz B, Goetz J and Labombard B 1995 *J. Nucl. Mater.* **220–222** 50
[15] Mayer M *et al* 1999 *J. Nucl. Mater.* **266–269** 604
[16] Matthews G *et al* 1997 *J. Nucl. Mater.* **241–243** 450
[17] Lipschultz B *et al* 1987 *J. Nucl. Mater.* **145–147** 15
[18] Samm U *et al* 1999 *J. Nucl. Mater.* **266–269** 616
[19] Mertens M *et al* 1997 *Nucl. Fusion* **37** 1607
[20] Rapp J *et al* 2000 *14th Int. Conf. on Plasma Surface Interactions (Rosenheim, May 2000) J. Nucl. Mater.* to be published
[21] Coster D *et al* 1999 *26th Eur. Phys. Soc. Conf. on Controlled Fusion and Plasma Physics (Maastricht, The Netherlands) Europhysics Conference Abstracts* vol 23J, p 1517
[22] Kallenbach A *et al* 1999 *J. Nucl. Mater.* **266–269** 343
[23] Kallenbach A *et al* 1999 *Plasma Phys. Control. Fusion* **41** 189
[24] Vietzke E and Haasz A A 1996 Chemical erosion *Physical Processes of the Interaction of Fusion Plasmas with Solids* ed W Hofer and J Roth (New York: Academic)
[25] Horn A *et al* 1994 *Chem. Phys. Lett.* **231** 193
[26] Roth J *et al* 1999 *J. Nucl. Mater.* **266–269** 51
[27] Vietzke E and Philipps V 1989 *Fusion Technol.* **15** 108
[28] Vietzke E *et al* 1982 *J. Nucl. Mater.* **111-112** 763
[29] Haasz T *et al* 1987 *J. Nucl. Mater.* **145–147** 412
[30] Pospiesczcyk A *et al* 1997 *J. Nucl. Mater.* **241–243** 833
[31] Poschenrieder W *et al* 1995 *J. Nucl. Mater.* **220** 36
[32] Stamp M D *et al* 2000 *14th Int. Conf. on Plasma Surface Interactions (Rosenheim, May 2000) J. Nucl. Mater.* to be published
[33] Philipps V, Pospieszczyk A, Erdweg M, Schweer B, Vietzke E and Winter J 1996 *Phys. Scr.* T **64** 71
[34] Monk R D *et al* 1999 *Phys. Scr.* T **81** 54
[35] Kallenbach A *et al* 1999 *Nucl. Fusion* **39** 901
[36] Vietzke E, Philipps V, Flaskamp K and Wild Ch 1987 *Amorphous Hydrogen Films* (Paris: Les Editions de Physique) p 351
[37] Ihde J *et al* 2000 *16th Int. Conf. on Plasma Surface Interactions (Rosenheim, May 2000) J. Nucl. Mater.* to be published
[38] Thoma A *et al* 1997 *Plasma Phys. Control. Fusion* **39** 1487
[39] Huber A *et al* 2000 *14th Int. Conf. on Plasma Surface Interactions (Rosenheim, May 2000) J. Nucl. Mater.* to be published
[40] Maier H *et al* 1999 *J. Nucl. Mater.* **266–269** 1003
[41] Unterberg B *et al* 1999 *J. Nucl. Mater.* **266–269** 75
[42] Lipschultz B *et al* 2000 *14th Int. Conf. on Plasma Surface Interactions (Rosenheim, May 2000) J. Nucl. Mater.* to be published
[43] Verbeek H, Stober J, Coster D P, Eckstein W and Schneider R 1998 *Nucl. Fusion* **38** 1789
[44] Rohde V *et al 16th Int. Conf. on Plasma Surface Interactions (Rosenheim, May 2000) J. Nucl. Mater.* to be published
[45] Ueda J *et al* 2000 *10th Workshop on Carbon Materials (Hohenkammer Castle, Germany, 18–19 September,*

2000) Phys. Scr. to be published
[46] Roth J, Bohdansky J and Wilson K L 1982 *J. Nucl. Mater.* **111–112** 775
[47] Philipps V, Flaskamp K and Vietzke E 1982 *J. Nucl. Mater.* **111–112** 781
[48] Philipps V *et al* 1995 *J. Nucl. Mater.* **220** 467
[49] Reichle R, Summers D D R and Stamp M F 1990 *J. Nucl. Mater.* **176–177** 375
[50] Philipps V, Pospieszczyk A, Esser H G, Kögler U, Mank G, Samm U, Schweer B and the TEXTOR team 1997 *J. Nucl. Mater.* **241–243** 105
[51] Fussmann G *et al* 1995 *Plasma Physics and Controlled Nuclear Fusion Research 1995 (Proc. 15th Int. Conf. (Seville 1995))* vol 2 (Vienna: IAEA)
[52] Kirschner A *et al* 2000 *Nucl. Fusion* **40** 989
[53] Naujoks D *et al* 1996 *Nucl. Fusion* **36** 671
[54] Krieger K *et al* 1999 *J. Nucl. Mater.* **266–269** 207
[55] Wienhold P *et al* 2000 *16th Int. Conf. on Plasma Surface Interactions (Rosenheim, May 2000) J. Nucl. Mater.* to be published
[56] Coad P *et al* 1999 *Phys. Scr.* T **81** 7
[57] Keudell A V *et al* 2000 *16th Int. Conf. on Plasma Surface Interactions (Rosenheim, May 2000) J. Nucl. Mater.* to be published
[58] von Seggern J *et al* 2000 *14th Int. Conf. on Plasma Surface Interactions (Rosenheim, May 2000) J. Nucl. Mater.* to be published
[59] Mayer M *et al* 2000 *14th Int. Conf. on Plasma Surface Interactions (Rosenheim, May 2000) J. Nucl. Mater.* to be published
[60] Rubel M *et al* 2000 *16th Int. Conf. on Plasma Surface Interactions (Rosenheim, May 2000) J. Nucl. Mater.* to be published
[61] Chankin A 2000 *14th Conf. on Plasma Surface Interactions (Rosenheim, Germany, May 2000) J. Nucl. Mater.* to be published
[62] Hawryluk R J *et al* 1979 *Nucl. Fusion* **19** 1307
[63] Nakamura H *et al* 1988 *Nucl. Fusion* **28** 43
[64] Rapp J *et al* 1997 *Plasma Phys. Control. Fusion* **39** 1615
[65] van Oost G *et al* 1995 *22th Eur. Phys. Soc. Conf. on Controlled Fusion and Plasma Physics (Bournemouth) European Conference Abstracts* vol 19c, part III, p 819
[66] Asmussen K *et al* 1998 *Nucl. Fusion* **38** 967
[67] Asmussen K *et al* 1997 *24th Eur. Phys. Soc. Conf. on Controlled Fusion and Plasma Physics (Berchtesgaden, 1997)* vol 21A, p 1393
[68] Tokar M 1997 *Nucl. Fusion* **37** 1691
[69] Post D E and Jensen R V *et al* 1977 *Atom. Data Nucl. Data Tables* **20** 397
[70] Steinbrink J *et al* 1997 *24th Eur. Phys. Soc. Conf. on Controlled Fusion and Plasma Physics (Berchtesgaden, 1997)* vol 21A, part IV, p 1809